Dislocation screening and strongly increased internal quantum efficiency in heteroepitaxial GaN/$Al_xGa_{1-x}N$ ultraviolet-emitting quantum wells

D. Fuhrmann, T. Retzlaff, M. Greve, L. Hoffmann, H. Bremers, U. Rossow, and A. Hangleiter*
Institute of Applied Physics, Technical University of Braunschweig, Mendelssohnstrasse 2, 38106 Braunschweig, Germany

P. Hinze and G. Ade
Physikalisch-Technische Bundesanstalt, Bundesallee 100, 38116 Braunschweig, Germany

(Received 7 August 2008; revised manuscript received 21 December 2008; published 12 February 2009)

While today's $Ga_xIn_{1-x}N$-based blue-light-emitting quantum wells exhibit internal quantum efficiencies in excess of 60%, ultraviolet structures at wavelengths shorter than 360 nm still are limited to efficiencies of a few percent. Recently, it was demonstrated that antilocalization of charge carriers due to energy barriers arising from sidewall quantum wells in V-shaped pits decorating dislocations is a key to understanding the high efficiency of $Ga_xIn_{1-x}N$-based quantum wells. Here we show that the unexpected presence of V-shaped pits in GaN/$Al_xGa_{1-x}N$ quantum wells leads to a dramatically increased internal efficiency of about 30%. In contrast, the efficiency of quantum wells with flat interfaces in the vicinity of dislocations remains very low.

DOI: 10.1103/PhysRevB.79.073303 PACS number(s): 78.55.Cr, 78.67.De, 81.05.Ea, 61.72.Ff

GaN-based light-emitting devices for the UV spectral region are of huge interest due to their potential use for water purification, sensor, or data storage applications. Recently, the realization of good quality $Al_xGa_{1-x}N$ layers with Al contents above 70% (Ref. 1) pushed the emission wavelength for nitride-based UV light-emitting diodes (LEDs) down to 250 nm. Even electroluminescence from an AlN LED at 220 nm was demonstrated.[2] Nevertheless the external quantum efficiency (EQE) for devices emitting below 365 nm is rather poor. Best values reported are in the range of 44% at 365 nm (Ref. 3) but only 1.1% at 352 nm (Ref. 4) for In-containing quantum wells (QWs) or 4% at 343 nm,[5] 1% at 280 nm,[6] and 0.01% at 250 nm (Ref. 1) for In-free QWs. In contrast $Ga_xIn_{1-x}N$-based violet/blue LEDs have best values above 70% for the internal quantum efficiency (IQE) at room temperature (RT).[7–10]

While the IQE reflects the quality of the active region, for the EQE also the light extraction efficiency and the injection efficiency are of importance. In nitrides, both IQE and EQE are limited by very high defect densities of around 1×10^9 cm^{-2}. For an active region based on $Ga_xIn_{1-x}N$ layers, the high IQE was most commonly attributed to a localization effect due to the formation of In-rich nanostructures as a consequence of phase separation within the $Ga_xIn_{1-x}N$ QWs.[11,12] It is argued that the mobile carriers get trapped and so localization can prevent the carriers from reaching the defects and recombine nonradiatively. Obviously this effect cannot take place for In-free structures and hence the poor efficiencies were thought to be the consequence. However, Smeeton *et al.*[13] could show that the In clustering sometimes seen in the transmission electron microscope (TEM) may be a consequence of experimental artifacts. Recently, Hangleiter *et al.*[14] proposed a mechanism based on thin sidewall QWs in V-shaped pits decorating dislocations that prevent carriers from nonradiative recombination and could explain the high IQE without a clustering effect. Due to an increased band gap around dislocations carriers get "antilocalized" such that they can move freely between dislocations but are prohibited from reaching the dislocation core by an energy barrier.[15] In fact, a very similar potential has been observed for other samples even without V-shaped pits but with reduced quantum well thickness close to dislocations.[16,17] Consequently, it appears possible to adopt this mechanism also for In-free GaN QWs and to achieve high efficiencies for such nitride-based UV emitters. Therefore we have grown GaN/$Al_xGa_{1-x}N$ SQWs, analyzed their microstructure in the vicinity of dislocations, and correlated the results with their internal quantum efficiency.

Several series of GaN/$Al_xGa_{1-x}N$ QW structures were grown by low-pressure metal-organic vapor phase epitaxy (MOVPE) using a horizontal reactor (AIX 200RF). TMGa, TMAl, and ammonia were used as precursors. All layers were grown with H_2 as the carrier gas and a total pressure of 50 mbar. On a sapphire substrate an AlN nucleation layer was deposited, followed by the $Al_xGa_{1-x}N$ buffer layer ($x_{Al}\approx23\%$), a GaN QW (1–4 nm), and an $Al_xGa_{1-x}N$ capping layer ($x_{Al}\approx28\%$). The buffer and capping layer were grown at 1190 °C and 1100 °C (thermocouple readings) with thicknesses of 800 and 70 nm, respectively. The single GaN QW was also grown at a lower temperature. The Al composition of the $Al_xGa_{1-x}N$ layers was measured by high-resolution x-ray diffraction (HXRD) and low-temperature (LT) photoluminescence (PL). For two samples we determined the QW width by TEM. For the optical measurements the samples were mounted in a helium cryostat for LT PL. As an excitation source we used a frequency-quadrupled Nd-YAG laser ($\lambda_{exc.}=266$ nm) with a high excitation power density ($P_{exc.}$ of several kW/cm^2, corresponding to an injection current density of the order kA/cm^2) for nonresonant excitation. In this case light is absorbed by the GaN QW and the $Al_xGa_{1-x}N$ barriers. Then transport of carriers from the barrier into the QW has to be considered. In contrast, under resonant excitation, carriers are only generated by light absorption in the QW, and thus only the optical properties of the QW are probed. Hence, we used an Ar-ion laser ($\lambda_{exc.}=335$ nm) with a much smaller absorbed power density only of the order 10 W/cm^2 for the resonant excitation. From the temperature- and excitation-power-dependent PL we deter-

 ©2009 The American Physical Society

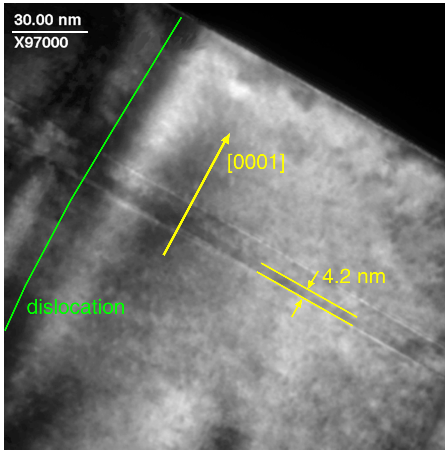

FIG. 1. (Color online) TEM image of a GaN/AlGaN single quantum well sample featuring regular and flat QW interfaces even close to dislocations (type A). The QW thickness is about 4.2 nm.

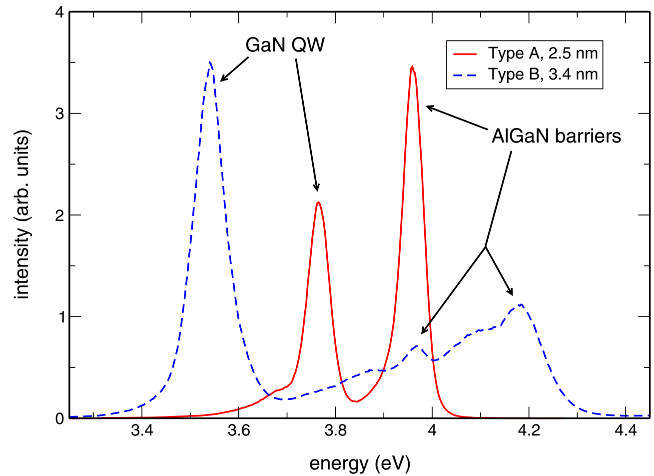

FIG. 3. (Color online) Low-temperature photoluminescence spectra under nonresonant excitation for two typical samples of types A and B. Besides the GaN QW emission, emission from barrier states can be seen.

mine the IQE. This method is valid if the IQE saturates for low temperature and for high excitation power. A detailed description of this method is published in Ref. 8. Cross-sectional transmission electron microscopy was carried out in a Philips CM 200 FEG microscope operated at 200 kV.

In the transmission electron microscope, two types of microstructures of the GaN/$Al_xGa_{1-x}N$ quantum well samples were found. The first type (type A), as shown in Fig. 1, exhibits nice flat quantum well interfaces, which remain completely regular even when intersecting a threading dislocation (atomic force microscopy reveals typical dislocation densities of the order 2×10^9 cm^{-2} for the $Al_xGa_{1-x}N$ buffer layers). In the case shown in Fig. 1, the quantum well has a thickness of 4.2 ± 0.2 nm. Such a structure would normally be regarded as an almost perfect quantum well.

On the other hand, the second microstructure type (type B), as depicted in Fig. 2, features well-defined V-shaped pits decorating essentially all dislocations (within the TEM field of view), irrespective of type (edge, screw, or mixed). The pit sidewalls are inclined by 61.5 degrees with respect to the *c* plane, as expected for the typical $(1\bar{1}01)$ facets forming the hexagonal inverted pyramids known as V-shaped pits[18] in $Ga_xIn_{1-x}N$/GaN quantum wells. The pit diameter is about 100–120 nm. The quantum well thickness amounts to about 2 nm on the *c* plane but only to about 1.1 nm on the pit sidewalls. From a simple geometric argument of deposition rates one would expect the ratio of thicknesses to be given by the cosine of the inclination angle, i.e., 0.48 in the present case. The observed ratio of 0.55 is slightly larger, indicating a modest lateral growth component for the quantum well.

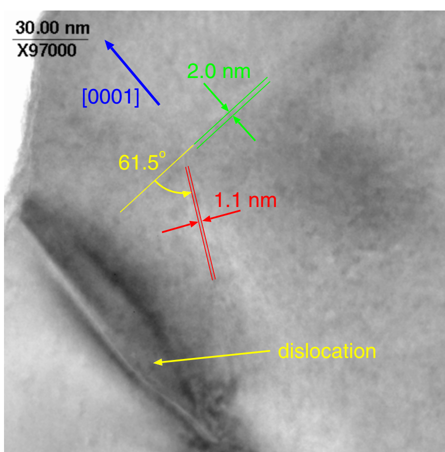

FIG. 2. (Color online) TEM image of a GaN/AlGaN single quantum well sample with dislocations decorated with V-shaped pits (type B). The QW thickness on the pit sidewalls is reduced to 1.1 nm from 2.0 nm for the *c*-plane wells.

Low-temperature photoluminescence spectra (nonresonant excitation) shown in Fig. 3 for two typical samples reveal the quantum well emission being subject to a strong shift due to the quantum confined Stark effect (QCSE).[19] In addition, the emission due to the $Al_xGa_{1-x}N$ barriers is observed, which is split in one case due to different Al content in the buffer and cap layers. As the narrow sidewall QWs of pits are close to the dislocations and thus subject to strong nonradiative recombination, their emission can only be observed in spatially resolved low-temperature measurements.[20]

Comparing the measured internal quantum efficiency under resonant excitation for the two types of samples (Fig. 4), we note that type A QWs suffer from an extremely rapid decrease in internal efficiency with increasing temperature, leaving almost no luminescence at room temperature and thus have very low IQE well below 1%. On the other hand, type B samples exhibit a much weaker decrease toward room temperature and remain highly efficient, with IQE values between 10 and 26% even under relatively weak pump power density. One should note that the IQE may reach its maximum value for different excitation power densities at low temperature and at room temperature.[8] Therefore the low-temperature IQE at constant excitation power as shown may not reach unity.

The temperature dependence of the IQE of the two types of samples was analyzed using a thermal activation model.[21]

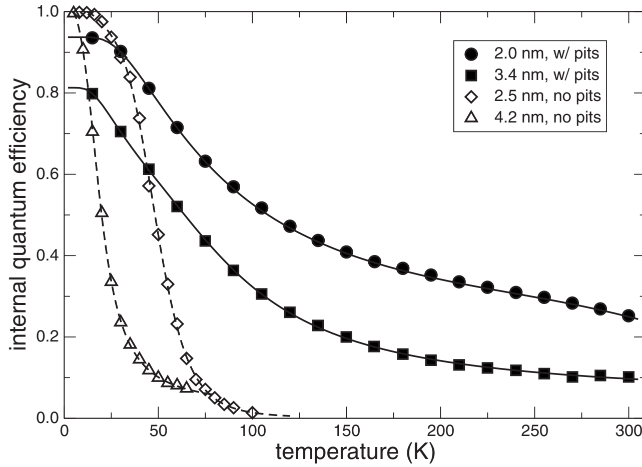

FIG. 4. Measured temperature dependence of the internal quantum efficiency for type A and type B samples (symbols), measured at a power density of about 5 W/cm^2. While type A samples have almost zero efficiency at room temperature, type B samples exhibit much higher efficiency at room temperature, reaching about 30% for the 2 nm sample. The full lines are fits using a thermal activation model. The activation energies derived from the fits are shown in Table I.

The results are summarized in Table I. Clearly, the activation energy can be collected into three groups, namely, energies below 10 meV, between 20 and 40 meV, and higher than 100 meV. Like in the case of $Ga_xIn_{1-x}N$ QWs,[8,21] the first group can be attributed to three-dimensional random localization, the second group coincides with the free exciton binding energy, and the third group is identified as an energy barrier. As the internal quantum efficiency can be written as

$$\eta_{\text{int}} = \frac{1}{1 + \frac{R_{\text{nonrad}}}{R_{\text{rad}}}}, \qquad (1)$$

where R_{nonrad} and R_{rad} are the nonradiative and the radiative recombination rates, respectively, the weighting factors of the exponentials represent the ratio of the nonradiative and the radiative probability. From Table I we note that weighting factors of the activation processes are lower for type B samples compared to type A as nonradiative recombination is suppressed. Moreover, within type B, wider wells show larger weighting factors due to reduced radiative oscillator strength.[19]

It is interesting to compare the thermal activation energies with the height of the potential barrier expected to arise from the narrow sidewall quantum wells of the V-shaped pits decorating and surrounding the dislocations. From the thicknesses of the QWs both on the c plane and on the $(1\bar{1}01)$ sidewalls of 2.0 and 1.1 nm, respectively, we can estimate the effective band gap in the sidewall QWs to be 150–200 meV higher than on the c plane. The barrier height thus corresponds closely the activation energy of 230 meV derived from the thermal activation analysis.

Obviously, optimized growth conditions tend to promote creation of pit structures both in $Ga_xIn_{1-x}N/GaN$ QW structures and in $GaN/Al_xGa_{1-x}N$ QWs. In the present case, the presence of pits leads to a dramatic enhancement of the internal efficiency even at rather low power density of a few W/cm^2. In terms of growth, it turns out that this was achieved by using similar growth conditions as for $Ga_xIn_{1-x}N$ QWs, namely, large V/III ratio and low temperature in the active region. Previously, reasonable internal efficiencies for UV-emitting QWs[22] were only possible at much higher power or current densities of the order kW/cm^2 or kA/cm^2, respectively, due to the quadratic increase in the radiative rate with carrier density.

Therefore it appears desirable to deliberately introduce V-shaped pits into UV-emitting quantum well structures in order to improve UV LED performance. To make maximum use of the pits, their size should be controlled to be large enough to screen dislocations, but as small as possible in order to leave as much active c-plane area as possible.

It is also interesting to consider the origin of relatively large efficiencies observed for quaternary InAlGaN UV-LEDs.[4] It is well known that growth conditions for $Ga_xIn_{1-x}N$ QWs, such as large V/III ratio, low growth temperature, and high pressure, tend to promote creation of V-shaped pits. Therefore it appears reasonable to assume that growth of InAlGaN QWs also has a tendency to inadvertently create pits and the companion thin sidewall quantum wells in the structures, leading to improved light-emission efficiency.

In conclusion, we have shown that $GaN/Al_xGa_{1-x}N$ quantum well structures exhibiting V-shaped pits decorating virtually all dislocations feature high internal quantum efficiency at room temperature. In contrast, very similar QWs with flat interfaces across dislocations suffer from very low efficiency. Thus "self-screening" of dislocations due to the formation narrow sidewall quantum wells within V-shaped

TABLE I. Thermal activation energies and weighting factors determined from fitting the temperature dependence of the IQE as shown in Fig. 4. The activation energy E_3 is significant in only one of the samples since the others have too low efficiencies.

Type	d_{QW} (nm)	E_{peak} (eV)	E_1 (meV)	A_1	E_2 (meV)	A_2	E_3 (meV)	A_3
A	2.5	3.765	5	16.4				
	4.2	3.482	6	1.28	26	398		
B	2.0	3.451	10	2.18	25	2.42	230	157
	3.4	3.389	5	1.41	27	17.5		

pits effectively suppresses nonradiative recombination not only in $Ga_xIn_{1-x}N$-based QWs but also in UV-emitting $GaN/Al_xGa_{1-x}N$ QWs.

The authors would like to acknowledge financial support of this work by the Deutsche Forschungsgemeinschaft (DFG).

*a.hangleiter@tu-bs.de

[1] V. Adivarahan, W. H. Sun, A. Chitnis, M. Shatalov, S. Wu, H. P. Maruska, and M. A. Khan, Appl. Phys. Lett. **85**, 2175 (2004).
[2] Y. Taniyasu, M. Kasu, and T. Makimoto, Nature (London) **441**, 325 (2006).
[3] D. Morita, M. Yamamoto, K. Akaishi, K. Matoba, K. Yasumoto, Y. Kasai, M. Sano, S.-I. Nagahama, and T. Mukai, Jpn. J. Appl. Phys., Part 1 **43**, 5945 (2004).
[4] H. Hirayama, K. Akita, T. Kyono, T. Nakamura, and K. Ishibashi, Jpn. J. Appl. Phys., Part 2 **43**, L1241 (2004).
[5] J. Edmond *et al.*, J. Cryst. Growth **272**, 242 (2004).
[6] W. Sun, V. Adivaharan, M. Shatalov, Y. Lee, S. Wu, J. Yang, J. Zhang, and M. A. Khan, Appl. Phys. Lett. **43**, L1419 (2004).
[7] S. Nakamura, M. Senoh, N. Iwasa, and S.-I. Nagahama, Appl. Phys. Lett. **67**, 1868 (1995).
[8] A. Hangleiter, D. Fuhrmann, M. Grewe, F. Hitzel, G. Klewer, S. Lahmann, C. Netzel, N. Riedel, and U. Rossow, Phys. Status Solidi A **201**, 2808 (2004).
[9] T. Mukai, M. Yamada, and S. Nakamura, Jpn. J. Appl. Phys., Part 1 **38**, 3976 (1999).
[10] D. Fuhrmann, C. Netzel, U. Rossow, A. Hangleiter, G. Ade, and P. Hinze, Appl. Phys. Lett. **88**, 071105 (2006).
[11] S. Chichibu, T. Azuhata, T. Sota, and S. Nakamura, Appl. Phys. Lett. **69**, 4188 (1996).
[12] Y. Narukawa, Y. Kawakami, M. Funato, S. Fujita, S. Fujita, and S. Nakamura, Appl. Phys. Lett. **70**, 981 (1997).
[13] T. M. Smeeton, M. J. Kappers, J. S. Barnard, M. E. Vickers, and C. J. Humphreys, Appl. Phys. Lett. **83**, 5419 (2003).
[14] A. Hangleiter, F. Hitzel, C. Netzel, D. Fuhrmann, U. Rossow, G. Ade, and P. Hinze, Phys. Rev. Lett. **95**, 127402 (2005).
[15] A. Hangleiter, C. Netzel, D. Fuhrmann, F. Hitzel, L. Hoffmann, H. Bremers, U. Rossow, G. Ade, and P. Hinze, Philos. Mag. **87**, 2041 (2007).
[16] S. Sonderegger, E. Feltin, M. Merano, A. Crottini, J. F. Carlin, R. Sachot, B. Deveaud, N. Grandjean, and J. D. Ganiere, Appl. Phys. Lett. **89**, 232109 (2006).
[17] N. K. van der Laak, R. A. Oliver, M. J. Kappers, and C. J. Humphreys, Appl. Phys. Lett. **90**, 121911 (2007).
[18] F. Scholz, A. Sohmer, J. Off, V. Syganow, A. Dörnen, J.-S. Im, A. Hangleiter, and H. Lakner, Mater. Sci. Eng., B **50**, 238 (1997).
[19] J. S. Im, H. Kollmer, J. Off, A. Sohmer, F. Scholz, and A. Hangleiter, Phys. Rev. B **57**, R9435 (1998).
[20] F. Hitzel, G. Klewer, S. Lahmann, U. Rossow, and A. Hangleiter, Phys. Rev. B **72**, 081309(R) (2005).
[21] S. Lahmann, F. Hitzel, U. Rossow, and A. Hangleiter, Phys. Status Solidi C **0**, 2202 (2003).
[22] H. Hirayama, J. Appl. Phys. **97**, 091101 (2005).